CHARACTERIZING THE OPTICAL PROPERTIES OF COASTAL WATERS USING FINE AND COARSE RESOLUTION

Brandon Casey, Neptune Sciences, Inc., 40201 Highway 190, Slidell, LA 70461

Robert Arnone, Naval Research Laboratory, Code 7333,

Stennis Space Center, MS 39529

Paul Martinolich, Neptune Sciences, Inc., 40201 Highway 190, Slidell, LA 70461

Sherwin Ladner, Planning Systems, Inc., Stennis Space Center, MS 39576

Marcos Montes, Naval Research Laboratory, Washington, DC 20375

David Kohler, Florida Environmental Research Institute, Tampa, FL 33611

W. Paul Bissett, Florida Environmental Research Institute, Tampa, FL 33611

ABSTRACT

Coastal optical properties derived from the ~ 1.1km resolution SeaWiFS satellite sensor were compared with those derived from NRL's ~ 9m resolution Portable Hyperspectral Imager for Low-Light Spectroscopy (PHILLS-2), an aircraft sensor flown during the LEO-15 2001 experiment off the coast of New Jersey. We defined the spatial variability within each 1.1km SeaWiFS pixel by using the PHILLS-2 data. Higher variability occurs in coastal waters and requires high resolution imagery to define coastal processes. This study illustrates how large scale imagery, such as SeaWiFS, under-samples the coastal optical properties.

The SeaWiFS data was atmospherically corrected using a modification of the NASA standard atmospheric correction method. A near-IR atmospheric correction method (Arnone, 1998) based on the assumption that normalized water-leaving radiance (L_{wn}) at 765nm and 865nm is not zero in the high turbid waters was applied. The PHILLS-2 data was atmospherically corrected using Tafkaa [4,7],a derivative of ATREM [4], to determine the remote sensing reflectance (R_{rs}). A flat fielding technique was applied to the R_{rs}. The flat-fielded R_{rs} was then converted to L_{wn}, and convolved with the SeaWiFS Spectral Response Function to produce R_{rs} at the SeaWiFS nominal band-centered wavelengths.

Identical bio-optical algorithms used in SeaWiFS processing were applied to both data sets to derive back-scattering (b_b). The imagery was then geo-rectified (SeaWiFS pixels were duplicated to match the resolution of the PHILLS-2 sensor) for direct comparison of the derived optical properties. Finally a smoothing technique was used to convert the PHILLS-2 pixels into SeaWiFS like pixels, as well as to approximate the variability in a single SeaWiFS pixel.

INTRODUCTION

Lower resolution sensors like SeaWiFS (and in the near future MODIS) are commonly used by those studying the ocean to derive ocean optical properties. The resolution of these sensors is appropriate for off-shore waters where the spatial variability

of ocean properties is low. But coastal waters respond to smaller scale processes and the optical properties are highly variable and are changing on both temporally short and spatially small scales. Higher resolution sensors are required to sense changing optical signatures which are influenced by processes such as river discharge of CDOM and sediments, dissipation and mixing of coastal waters offshore, re-suspension of bottom sediments from tidal currents and wind wave forcing, and local phytoplankton blooms and decay. High resolution imagery is required to detect the variability of these coastal optical properties in addition to providing an understanding of how these optical properties are integrated into larger scale imagery which are commonly used (such as SeaWiFS).

The back-scattering (b_b) derived from the ~ 1.1km resolution SeaWiFS satellite sensor was compared with b_b derived from NRL's ~ 9m resolution Portable Hyperspectral Imager for Low-Light Spectroscopy (PHILLS-2), an aircraft sensor flown during the LEO-15 2001 experiment off the coast of New Jersey. Approximately one hour lapsed between the SeaWiFS pass and the PHILLS-2 data collection flight. The increased resolution of the PHILLS-2 sensor was used to show that SeaWiFS inadequately defines the coastal optical properties due to the intra-pixel variability inherent in its 1.1km resolution pixels. The variability of optical properties increases directly with the magnitude of the property. The coastal region therefore should have higher variability than offshore waters. By using different spatial sensors we will define this variability in coastal/near-shore and offshore waters.

The LEO-15 site represents a large variety of water optical types which were highly sampled during the 2001 experiment. A time-series of SeaWiFS derived optical products is commonly used to monitor and understand coastal upwelling and development of phytoplankton blooms in response to seasonal cycles. This comparison study of high and low resolution scales will improve the understanding of the time-series in coastal waters. For example, when comparing ground truth with SeaWiFS values, the spatial variability of the 1.1km region must be considered.

SeaWiFS and PHILLS-2 imagery were processed using different procedures to produce similar spectral remote sensing reflectance, which was used in identical in-water optical algorithms. The imagery was then geo-rectified (SeaWiFS pixels were duplicated to match the resolution of the PHILLS-2 sensor) for direct comparison of the derived optical properties. Finally a smoothing technique was used to convert the PHILLS-2 pixels into SeaWiFS like pixels, as well as to approximate the variability in a single SeaWiFS pixel.

SEAWIFS PROCESSING

The SeaWiFS data was processed using the Automated Processing System [6] Version 2.4 developed by the Naval Research Laboratory (NRL). The Automated Processing System (APS) is a collection of software programs assembled by NRL which handles complete processing of satellite imagery after reception including atmospheric correction, the application of bio-optical algorithms to derive optical properties, and warping of the imagery to a standard map. APS implements a modification of the NASA SeaDAS (v4.0) atmospheric correction procedures (Gordon and Wang, 1998). The modification introduces a near-IR atmospheric correction method [1] based on the

assumption that L_{wn} at 765nm and 865nm is not zero in the high turbid waters. This is an iterative application of an atmospheric and ocean optical model to separate atmospheric aerosols and water reflectivity in coastal waters.

The Arnone back-scattering (b_b) at 555nm algorithm is based on the following semi-analytical algorithm:

Equation 1

$$R_{rs}(670nm) = 0.051 * \frac{b_b(670nm)}{a_t(670nm) + b_b(670nm)}$$

$$where\ a_t(670nm) = a_w(670nm) - a_{phi}(670nm) + a_{CDOM}(670nm)$$

a_{phi} = chorophyll absorption

a_{CDOM} = CDOM absorption

a_w = water absorption

a_{phi} was estimated from the NASA OC_4 algorithm, and a_{CDOM} from an $R_{rs}(555nm) \rightarrow R_{rs}(670nm)$ regression. $b_b(670nm)$ was solved for based on $R_{rs}(670nm)$.

PHILLS-2 PROCESSING

The PHILLS-2 sensor was flown on a Citation aircraft at an altitude of approx. 30,000 ft. over the LEO-15 site off the coast of New Jersey. The PHILLS-2 data set was collected by flying 14 mapping runs in the east-west direction with every other run being used for calibration. This produced 7 lines of data for research. The approximate length of each flight line was about 65km. Each flight line was collected in approximately 7 minutes, with the entire data set being collected in approximately 1.5 hours (calibration runs were not complete runs and were done while turning). The flight lines were collected from 0900 to 1030 local time July 31, 2001, about one hour after the SeaWiFS pass, with a solar altitude between 35 to 50 degrees. The data was processed and calibrated by the methods described in Kohler et al. 2002 [5] using the March 2002 calibration values.

The PHILLS-2 sensor suffers from a spectral "smile". The spectral smile is a consequence of the PHILLS-2 sensor employing a grating spectrograph, which is the cause of a change of dispersion angle with field position, i.e. the sensor does not respond to the same wavelength across the scan-line. In an attempt to repair the damages caused in part by this "smile", but also attributable to insufficient radiometric calibration or insufficient cross-track angular considerations during atmospheric correction, a flat fielding technique (described below) was applied to the R_{rs}. The flat-fielded R_{rs} was then converted to L_{wn}, and convolved with the SeaWiFS Spectral Response Function (described below) to produce R_{rs} at the SeaWiFS nominal band-centered wavelengths (412nm, 443nm, 490nm, 510nm, 555nm, 670nm). The PHILLS-2 is a hyperspectral sensor with ~ 4nm spacing between channels, where as SeaWiFS has approximately 20nm channel spacing.

PHILLS-2 ATMOSPHERIC CORRECTION

The PHILLS-2 raw radiance values were atmospherically corrected using Tafkaa [7]. The *mid latitude summer* atmospheric model was selected and ozone and wind speed values from EPTOMS (Earth Probe Total Ozone Mapping Spectrometer) and NCEP (National Center for Environmental Prediction) respectively were included in the Tafkaa configuration file. Additionally options were chosen to direct Tafkaa to select an aerosol model in pixel-by-pixel mode and to produce R_{rs} as its output.

FLAT-FIELDING TECHNIQUE

In very off-shore waters it is assumed that the R_{rs} is uniform (a flat field). If we can approximate the actual R_{rs} for very off-shore waters, we can calculate a correction scalar for each pixel across a scan line. Since the PHILLS-2 sensor is a pushbroom type sensor, the correction scalars for each scan pixel should be consistent for an entire run, and we can traverse the run line by line multiplying each pixel by its respective correction scalar to get a more accurate approximation of the actual R_{rs}.

To approximate the actual R_{rs}, PHILLS-2 R_{rs} was compared with SeaWiFS R_{rs}, and by observation it was determined that the mid left-hand side of the PHILLS-2 scan-line[1] most closely aligned with the SeaWiFS values. Based on these observations, a box was defined covering very off-shore waters from this left-hand side of each PHILLS-2 run such that the values contained in the box were near SeaWiFS values and were mostly uniform throughout (see *Table 1*). These boxes were used to flat-field the Tafkaa corrected PHILLS-2 bands. The values contained in the box were averaged and used as our R_{rs} approximation for flat-fielding. Next a line was chosen very off-shore where the flat-field assumption could be made. This line and a number of its neighbors were averaged in the along track direction and used to determine a correction scalar for each pixel on the line such that when multiplied by the R_{rs} value the result would equal our approximated R_{rs}. This two-dimensional array of correction scalars (one for each pixel across the scan line of every band), our flat-fielding function, could then be applied to an entire run to generate a more accurate estimate of R_{rs}.

Table 1: Box Parameters (isp = starting pixel, iep = ending pixel, isl = starting line, iel = ending line, line = line number of flat field, lines = number of following lines averaged with line).

Run	Isp	iep	isl	iel	line	numlines
002	546	595	631	680	631	50
004	454	503	5446	5490	5446	45
006	546	595	1251	1301	1251	51
008	494	595	7024	7077	7024	54
010	546	595	94	143	94	50
012	546	595	6950	7000	6950	50
014	523	591	485	600	485	116

[1] When viewing in the along track direction. There is a stripe with a width of about eight pixels on one side of a scan-line most probably caused by some object obstructing the PHILLS-2 lens. The left-hand side is the side opposite this stripe.

Note that, the box average and the correction scalars were calculated in log space[2] and hence the R_{rs} values should be converted to log space before multiplying by the correction scalars. *Equation 2* was used to convert values into log space, and *Equation 3:* Used after flat-fielding to convert the flat-fielded $\acute{R}rs$ out of log space. was used to convert out of log space. Also, since we were dealing with atmospherically corrected R_{rs}, some values were negative due to overcorrection by Tafkaa. We tried to recover from this in two ways. First, all R_{rs} values were shifted into the positive by adding an amount to them before taking the log. The values would then have this amount subtracted after applying the correction scalar and shifting back out of log space. Since the maximum value of $R_{rs} = \frac{1}{\pi}$ [7] and $\frac{1}{\pi} \approx .32$, this value was chosen to ensure that all values were shifted into the positive (*See Equation 2* and *Equation* 3: Used after flat-fielding to convert the flat-fielded $\acute{R}rs$ out of log space.). Second, any R_{rs} that was still negative after flat-fielding was set to the average of all positive R_{rs} on the same line. Although it may have been more appropriate to use the average of the neighbors in a 3x3 or 5x5 box, for programming simplicity the values on a single line were used. It is assumed that the PHILLS-2 sensor is of high enough resolution that values on a single line are spatially close enough to make the average an acceptable approximation.

Equation 2

$$R'_{rs} = \log_{10}\left(R_{rs} + .32\right)$$
$$R_{rs} = 10^{R'_{rs}} - .32$$

Equation 3: Used after flat-fielding to convert the flat-fielded $\acute{R}_{rs}$ out of log space.

The flat-fielding procedure was applied to each run.

SPECTRAL CONVOLUTION TO SEAWIFS CHANNELS

The flat-fielded R_{rs} was converted to L_{wn} using *Equation 4*.

[2] Based on Wang's decision to perform his interpolations in log space for out-of-band correction of SeaWiFS L_{wn} [9].

Equation 4

$$R_{rs} = \frac{L_{wn}}{E_0}$$

where L_{wn} is normalized water - leaving radiance

E_0 is incident solar irradiance

L_{wn} values were then multiplied by the SeaWiFS Spectral Response Function (SRF) [8] using the following equation:

Equation 5

$$\langle L_{wn}(\lambda)\rangle = \frac{\int L_{wn}(\lambda) S_i(\lambda) d\lambda}{\int S_i(\lambda) d\lambda}$$

where S_i is the SeaWiFS SRF for band *i* at a nominal center wavelength λ_i [9]. The SeaWiFS SRF is defined for wavelengths from 380nm to 1150nm with 1nm spacing. Log-linear interpolation was used to approximate the PHILLS-2 response at the SeaWiFS SRF wavelengths. For SeaWiFS SRF wavelengths outside of the PHILLS-2 range, one of two methods was used to approximate the PHILLS-2 response. If the SeaWiFS SRF wavelength was less than the lowest PHILLS-2 wavelength, then the response at that wavelength was set to the response at the lowest PHILLS-2 wavelength. If the SeaWiFS SRF wavelength was greater than the highest PHILLS-2 wavelength, then the PHILLS-2 response at 1150nm was set to a fraction of the response at the highest PHILLS-2 wavelength and log-linear interpolation was used to approximate the values between them. The fraction is based on Barnes's suggestion [1] of setting the response at 1150nm equal to 1/3 of the response at 850nm. This fraction was interpolated to the highest PHILLS-2 wavelength (964.121nm) and found to be ~ .4466.

Equation 6

$$L_{wn}(\lambda_i) = \begin{cases} L_{wn}(\Lambda_1) & ,380 \le \lambda_i \le \Lambda_1 \\ \text{interpolate} & ,\Lambda_1 \le \lambda_i \le \Lambda_{122} \\ L_{wn}(1150) = & \\ .4466 * L_{wn}(\Lambda_{122}) & ,\Lambda_{122} \le \lambda_i \le 1150 \\ \text{interpolate} & \end{cases}$$

Equation 6 provides a mathematical formula for the interpolation of the PHILLS-2 L_{wn} from the PHILLS-2 wavelengths to L_{wn} at the SeaWiFS SRF wavelengths, where λ_i is the SeaWiFS SRF wavelength and Λ_I is the wavelength of PHILLS-2 band *I*.

Next the SeaWiFS out-of-band correction [9] was applied to convert the SeaWiFS derived $\langle L_{wn}\rangle$ to $[L_{wn}]$ at the SeaWiFS nominal band-centered wavelengths. The $[L_{wn}]$ values were converted to R_{rs} using the Tafkaa calculated extraterrestrial solar irradiance (see *Equation 4*).

PHILLS-2 OPTICAL PRODUCT CREATION, GEOMETRIC REGISTRATION

The b_b product was created using identical algorithms used in SeaWiFS processing and the PHILLS-2 data set was geo-rectified using tools developed for the APS. This allowed us to warp the PHILLS-2 and SeaWiFS data sets to the same map covering the LEO-15 site so that a direct comparison could be made. APS tools were leveraged where possible to accelerate PHILLS-2 processing and research.

SMOOTHING TECHNIQUE (PHILLS-2 → SEAWIFS RESOLUTION)

To demonstrate the variability in a single SeaWiFS pixel, the PHILLS-2 b_b product was spatially averaged using a 109x109 pixel box to convert our ~ 10m resolution map to the ~ 1.1km resolution of SeaWiFS. Essentially, we made SeaWiFS pixels. In addition, for each pixel, the standard deviation and the maximum and minimum value were calculated in the box. So for each pixel in our original 10,000 X 5,000 pixel warped map, four values were produced. The first value was the mean of the values contained in our 109 X 109 pixel box. The second value was the standard deviation of those values. And the third and fourth values were the largest and smallest values in our 109 X 109 pixel box, referred to as the maximum and minimum respectively.

RESULTS

The PHILLS-2 back-scattering at 555nm matched up excellently with SeaWiFS back-scattering at 555nm. Back-scattering from SeaWiFS and PHILLS-2 using the Arnone algorithm at 555nm is shown in Figures 1 and 2, note the identical linear color scale! The off-shore front follows the same pattern for both sensors, although it has receded further off-shore in the ~ 1hr delayed PHILLS-2 data. Magnificent, detailed river plumes and eddies can be seen in-shore in the PHILLS-2 data. We can see that the discharge from the Great Bay moves South after entering the Atlantic, while discharge from the Absecon inlet exits in two plumes and remains close to the coast. Nothing recognizable can be discerned from the SeaWiFS data in-shore.

The spatially averaged b_b product when compared with SeaWiFS has a correlation coefficient of .752. The slope and y-intercept of the best-fit line are .612 and .003 respectively with SeaWiFS on the X-axis and PHILLS-2 on the Y-axis (see figures 3 and 5).

In order to study the effects of intra-pixel variability of SeaWiFS in off-shore and coastal waters, we partitioned our map. By observation we decided to classify coastal waters as those waters having a B_b greater than .011 m^{-2}, and all others as off-shore waters. The average standard deviation of our coastal waters was found to be .0106, and for off-shore waters .0026. This is an approximation of the average standard deviation in a single SeaWiFS pixel for waters of two different turbidity levels and is in-line with our expectations of higher variability in coastal waters than off-shore. Figure 6 is a cross-section of the standard deviation image (line 2980), the plot moves left to right from coastal to off-shore waters. We can see from this image that the standard deviation fluctuates more and has higher values in coastal waters and becomes much flatter as we

move into off-shore waters (see also figure 7). The mean (of the already smoothed pixels) for coastal waters was found to be .025 and for off-shore waters to be .008. What this means is that for a single SeaWiFS pixel with a value of .025, the range of values that fall within one standard deviation could be as large as 50% greater or smaller than .025. Another way to look at this is to look at the average difference between the maximum and the minimum value found in our 109 x 109 pixel boxes, which was found to be .09 for coastal waters and .022 for off-shore waters. So on average in these coastal waters the maximum value of b_b in a single SeaWiFS pixel was .09 greater than the minimum value of b_b, a difference almost 4 times greater than our coastal average.

CONCLUSION

The PHILLS-2 b_b and the SeaWiFS b_b show excellent agreement! This is the first time that optical products have been generated at different resolutions with very similar results. The error differences of the two sensor's resolution can be explained by the spatial variability of the optical properties of the sensors. The methods used in calibration, atmospheric correction, and retrieval of remote sensing reflectance were completely different for the two sensors, yet the results are very similar. This suggests that the radiometric control and quantitative analyses is being applied correctly. These results pave the way for continued research in understanding coastal optical properties through remote sensing.

The comparison of spatial scales of the optical properties at 1.1km and 9m clearly indicates the high variability of back-scattering occurring in coastal waters. The results expose the limitations of SeaWiFS for characterizing coastal processes. The simulation of SeaWiFS b_b from PHILLS-2 b_b indicates that a significant variability of optical properties occurs within a 1.1km SeaWiFS pixel. The variability is directly proportional to the magnitude of the mean values (see figure 8). This indicates that in ground-truthing of optical properties for validation of algorithms, the range of the optical product is linked with the pixel resolution and the magnitude of the property. The validation of coastal optical algorithms must consider this spatial variability.

Although the PHILLS-2 sensor is still under active development, by using our flat-fielding technique and convolving to SeaWiFS response bands, we have been able to get some results that match up well with SeaWiFS. By applying a smoothing technique we have been able to approximate the SeaWiFS response based on PHILLS-2 data and have shown that significant intra-pixel variability exists. This intra-pixel variability information is lost when using lower resolution sensors such as SeaWiFS. For coastal waters, this can be significant and can cause feature loss.

The infrastructure developed in the APS was leveraged to accelerate the processing of the PHILLS-2 data. We have constructed the code for satellite and aircraft ocean color processing so that similar algorithms and processing methods can be easily applied to several sensors for comparison and algorithm tuning for different sensors.

REFERENCES

1. Arnone, R. A., P. Martinolich, R. W. Gould, R. Stumpf, and S. Ladner, 1998: Coastal Optical Properties Using SeaWiFS. SPIE Ocean Optics XIV.

2. Barnes, R.A., W.E. Esaias, and C.R. McClain, 1995: "A Proposed On-Orbit, Out-of-Band Correction Scheme for SeaWiFS." In McClain, C.R., K. Arrigo, W.E. Esaias, M. Darzi, F.S. Patt, R.H. Evans, J.W. Brown, C.W. Brown, R.A. Barnes, and L. Kumar, 1995: SeaWiFS Algorithms, Part 1, *NASA Tech. Memo. 104566, Vol. 28*, S.B. Hooker and E.R. Firestone, Eds., NASA Goddard Space Flight Center, Greenbelt, Maryland, 20-25.

3. Davis, C.O., J. Bowles, R.A. Leathers, D. Korwan, T.V. Downes, W.A. Snyder, W.J. Rhea, W. Chen, J. Fisher, W.P. Bissett, and R.A. Reisse, 2002: Ocean PHILLS Hyperspectral Imager: Design, Characterization, and Calibration. *Optics Express*, **10**, 210-221.

4. Gao, Bo-Cai, Marcos J. Montes, Ziauddin Ahmad, and Curtiss O. Davis, 2000: Atmospheric Correction Algorithm for Hyperspectral Remote Sensing of Ocean Color From Space. *Applied Optics*, **39**, 887-896.

5. Kohler, D., W. P. Bissett, C. O. Davis, J. Bowles, D. Dye, R. G. Steward, J. Britt, M. Montes, O. Schofield, and M. Moline. 2002: High Resolution Hyperspectral Remote Sensing Over Oceanographic Scales at the LEO-15 Field Site. SPIE Ocean Optics XVI.

6. Martinolich, P., APS User's Guide Version 2.4. November 2001.

7. Montes, M., Bo-Cai Gao. Tafkaa User's Guide Version 2002 April 23 for Tafkaa Version 2002-04-23.

8. SeaWiFS Spectral Response Function obtained from http://seawifs.gsfc.nasa.gov/SEAWIFS/RECAL/Repro4/atmospheric_correction.html

9. Wang, M., B.A. Franz, R.A. Barnes, and C.R. McClain, 2000: Effects of Spectral Bandpass on SeaWiFS-Retrieved Near-Surface Optical Properties of the Ocean. *Applied Optics*, **40**, 343-348.

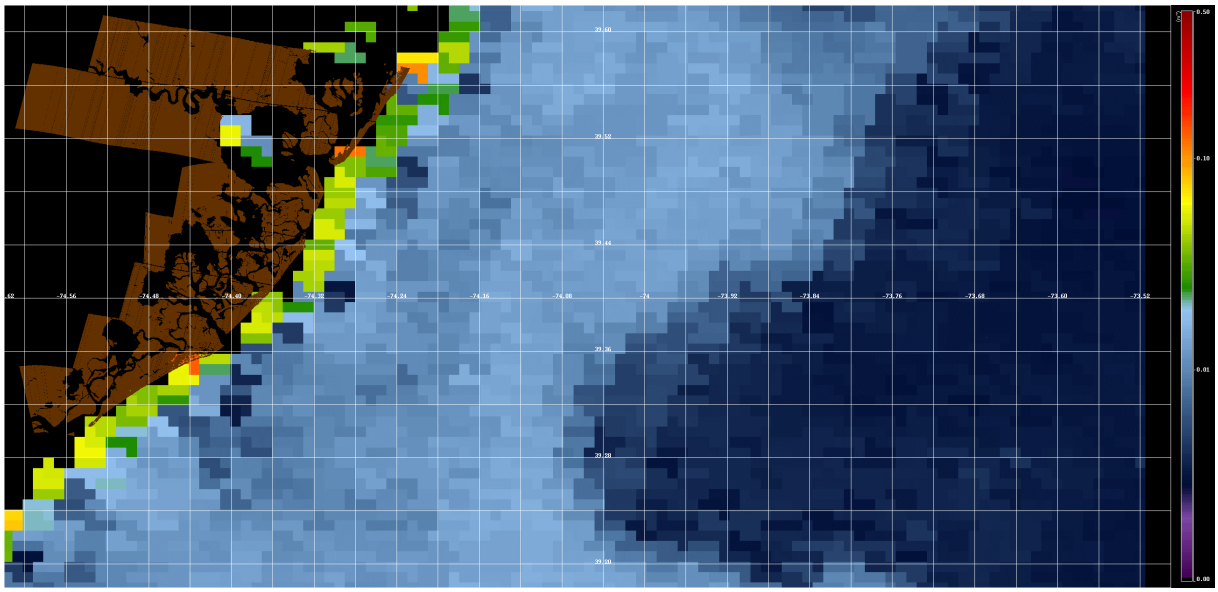

Figure 1: SeaWiFS b_b at 555nm Arnone algorithm. Log scaling from .001 to .5 m^{-2}.

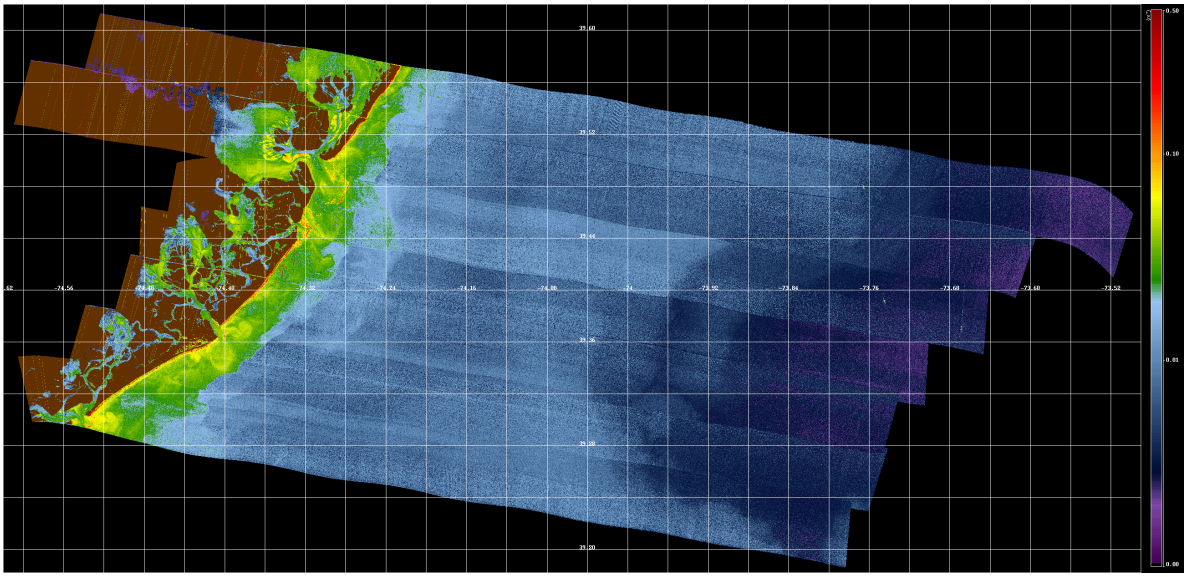

Figure 2: PHILLS-2 b_b at 555nm Arnone algorithm. Log scaling from .001 to .5 m^{-2}.

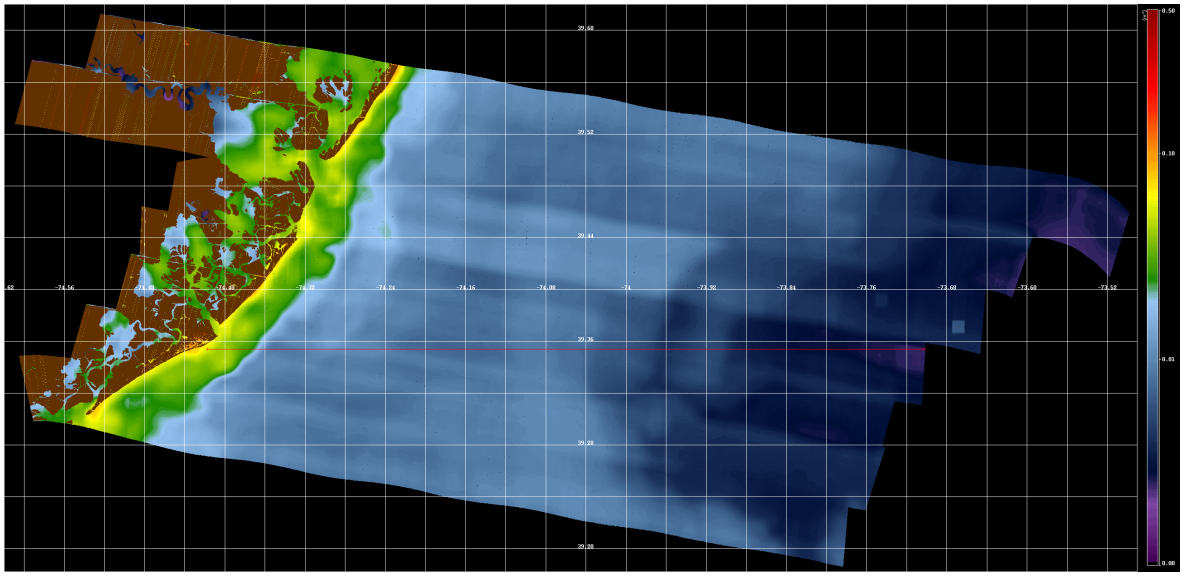

Figure 3: PHILLS-2 b_b Arnone algorithm spatially averaged using a 109 x 109 pixel box. The red horizontal line near center of the image indicates where the profile was taken for the overlays in figure 7. Log scaling from .001 to .5 m^{-2}.

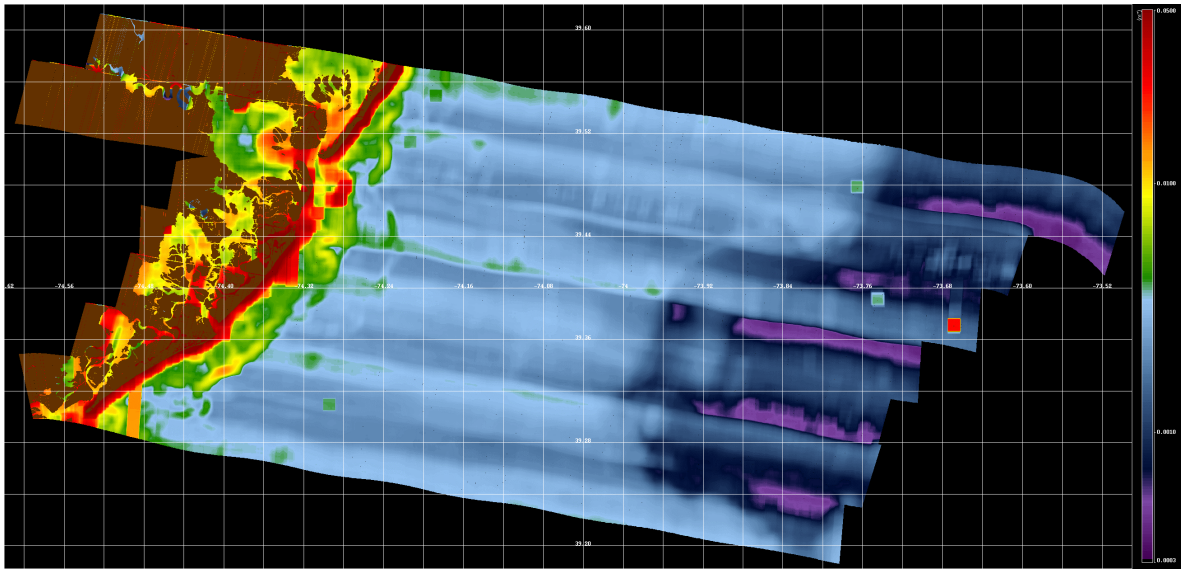

Figure 4: PHILLS-2 b_b Arnone algorithm, standard deviation in 109 x 109 pixel box. Log scaling from .0003 to .03 m^{-2}.

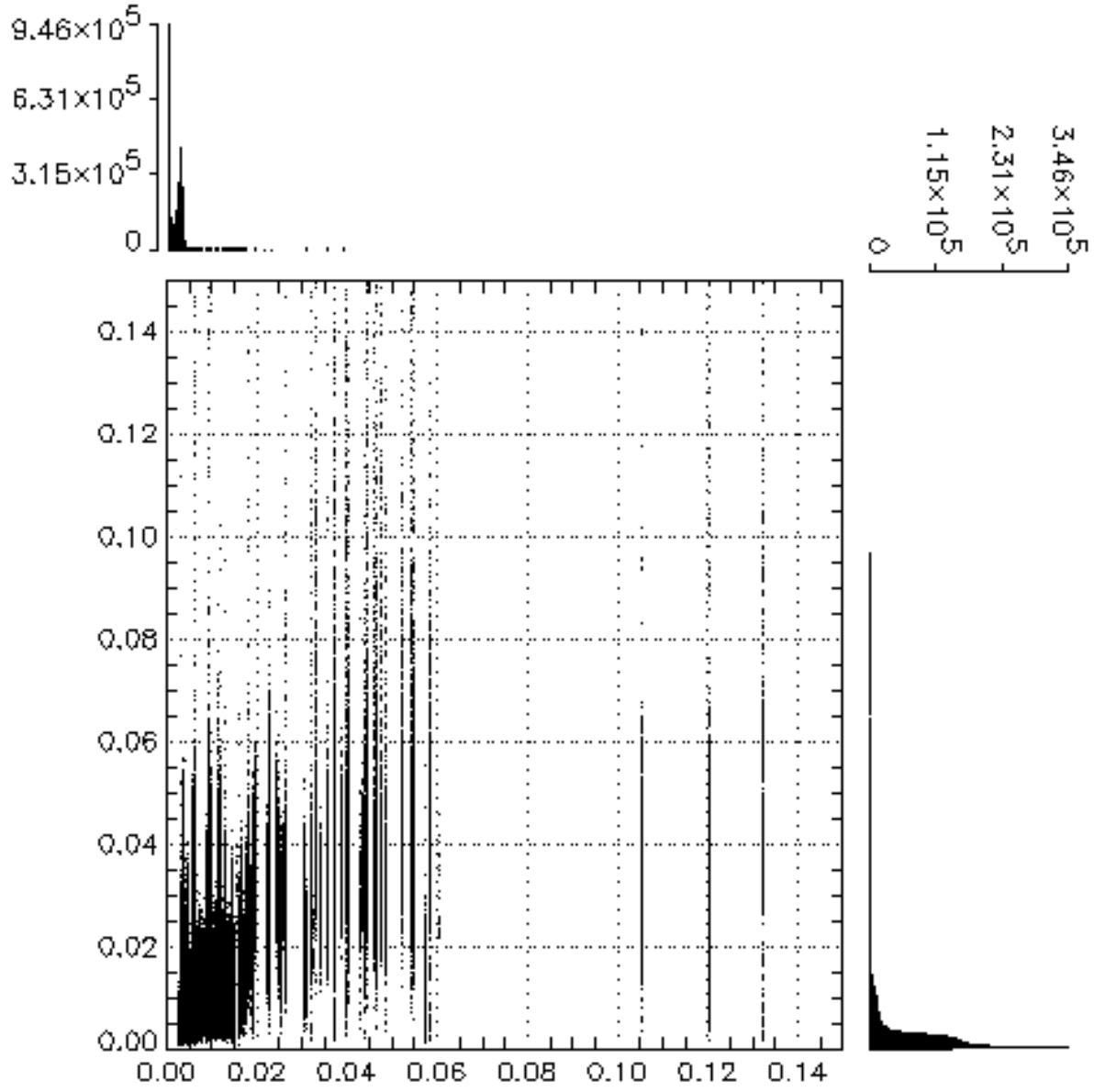

Figure 5: Scatter plot of PHILLS-2 b_b (y-axis) vs. SeaWiFS b_b (x-axis) with corresponding histograms to the right (PHILLS-2) and top (SeaWiFS) showing the distribution of values. There is a correlation of .752 between PHILLS-2 and SeaWiFS b_b and a slope and y-intercept of .612 and .003 respectively.

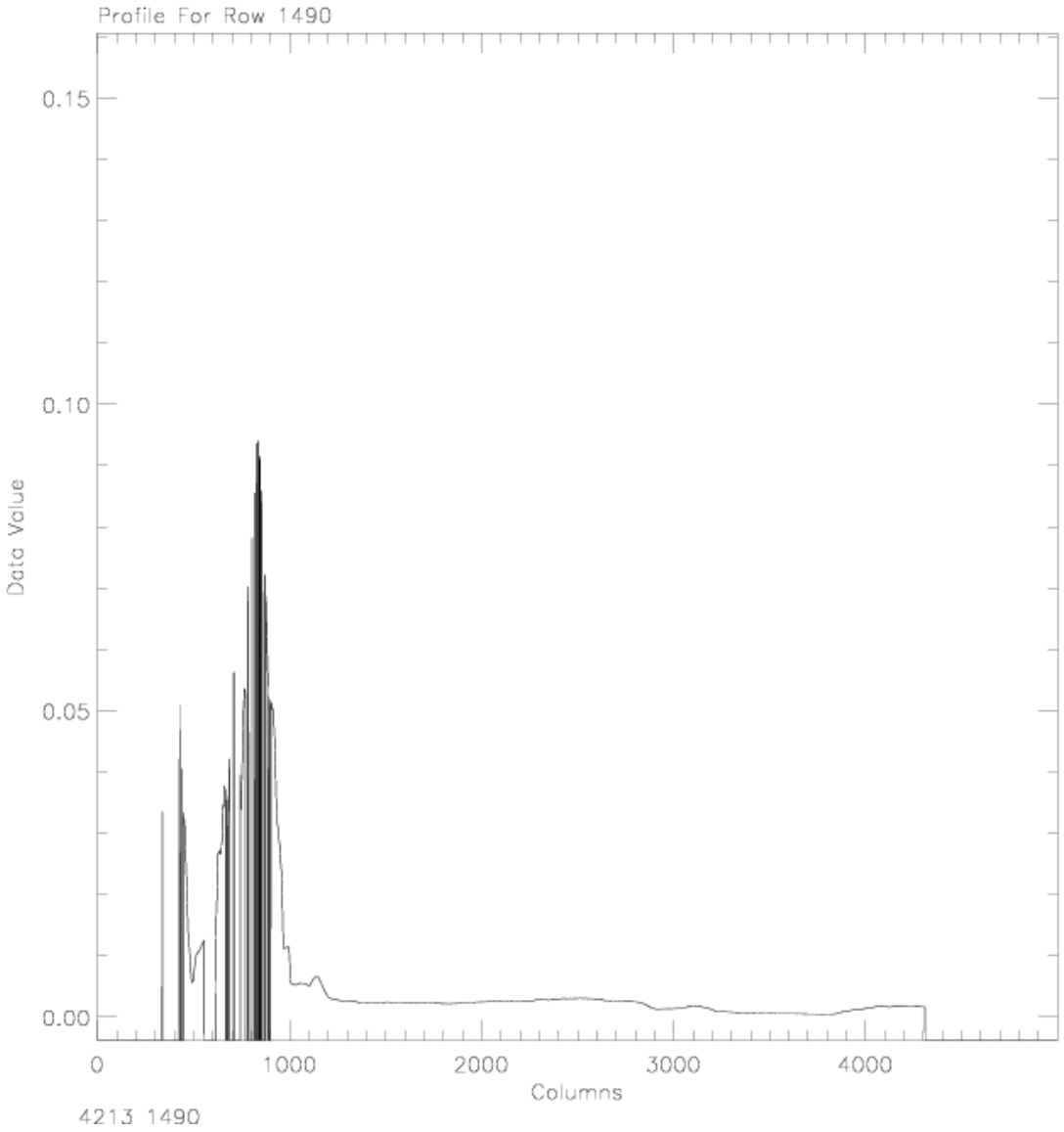

Figure 6: Profile of line 2980 from figure 4 showing a decrease in the variability and magnitude of the standard deviation of b_b as we move left to right from coastal to off-shore waters.

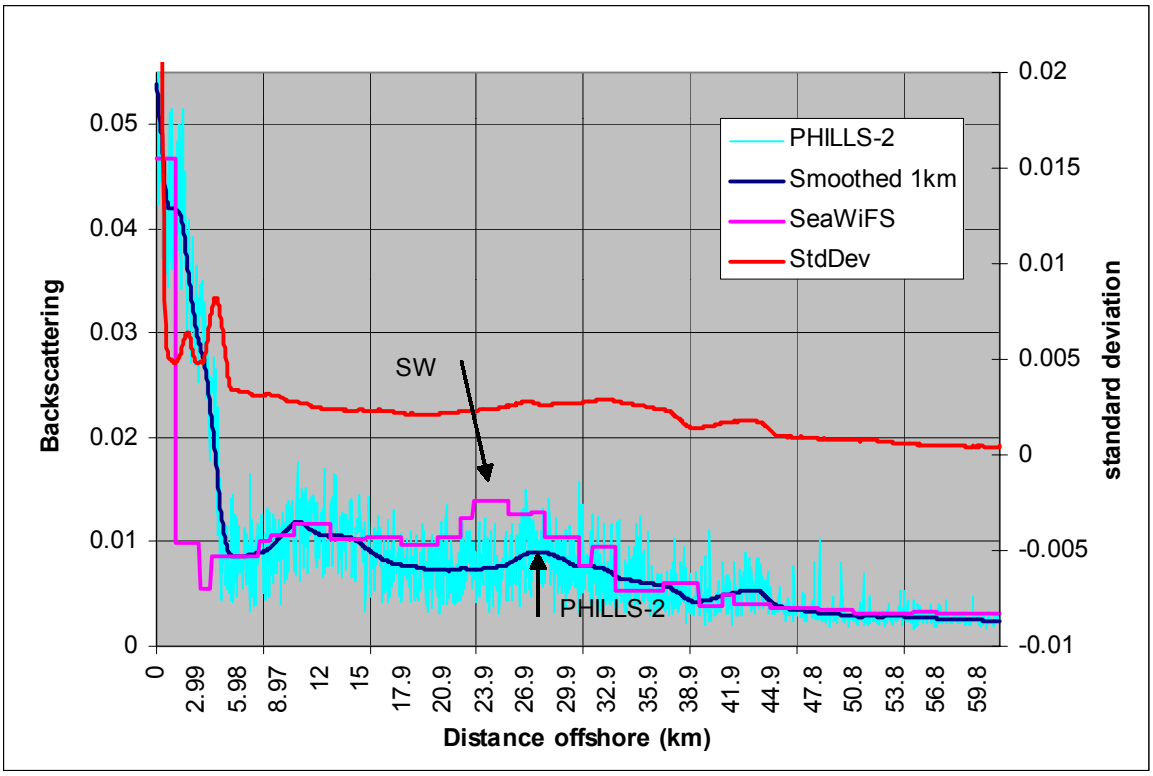

Figure 7: Overlay of PHILLS-2 b_b, PHILLS-2 b_b smoothed using 109 x 109 pixel box, SeaWiFS b_b, and PHILLS-2 b_b standard deviation of 109 x 109 pixel box, showing excellent agreement between SeaWiFS and PHILLS-2. These profiles were taken from line 3040 (red line in figure 3). The scaling on the left is for the three b_b lines, and the scaling on the right is for the standard deviation product. The arrows marked "SW" and "PHILLS-2" highlight the shift in the front observed due to the ~1hr delayed PHILLS-2 data collection.

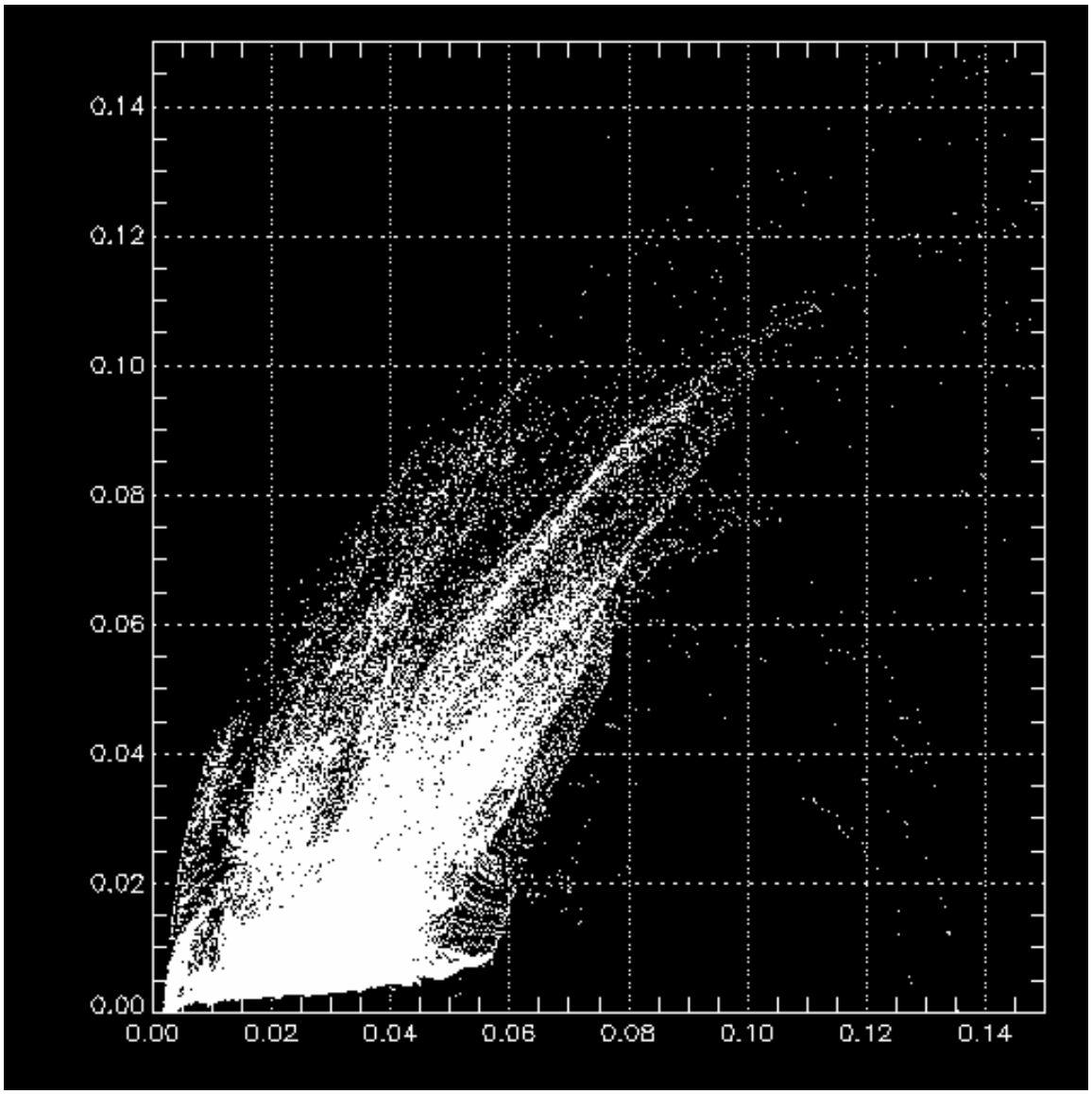

Figure 8: Scatter plot of PHILLS-2 b_b standard deviation of 109 x 109 pixel box (y-axis) and b_b smoothed using a 109 x 109 pixel box (x-axis) showing increasing standard deviation with increasing mean.